Quantitative pharmacology approaches to inform treatment strategies against tuberculosis

Mehta, K.

Section II.

Quantitative Pharmacology Approaches for First-Line Anti-Tuberculosis Therapeutic

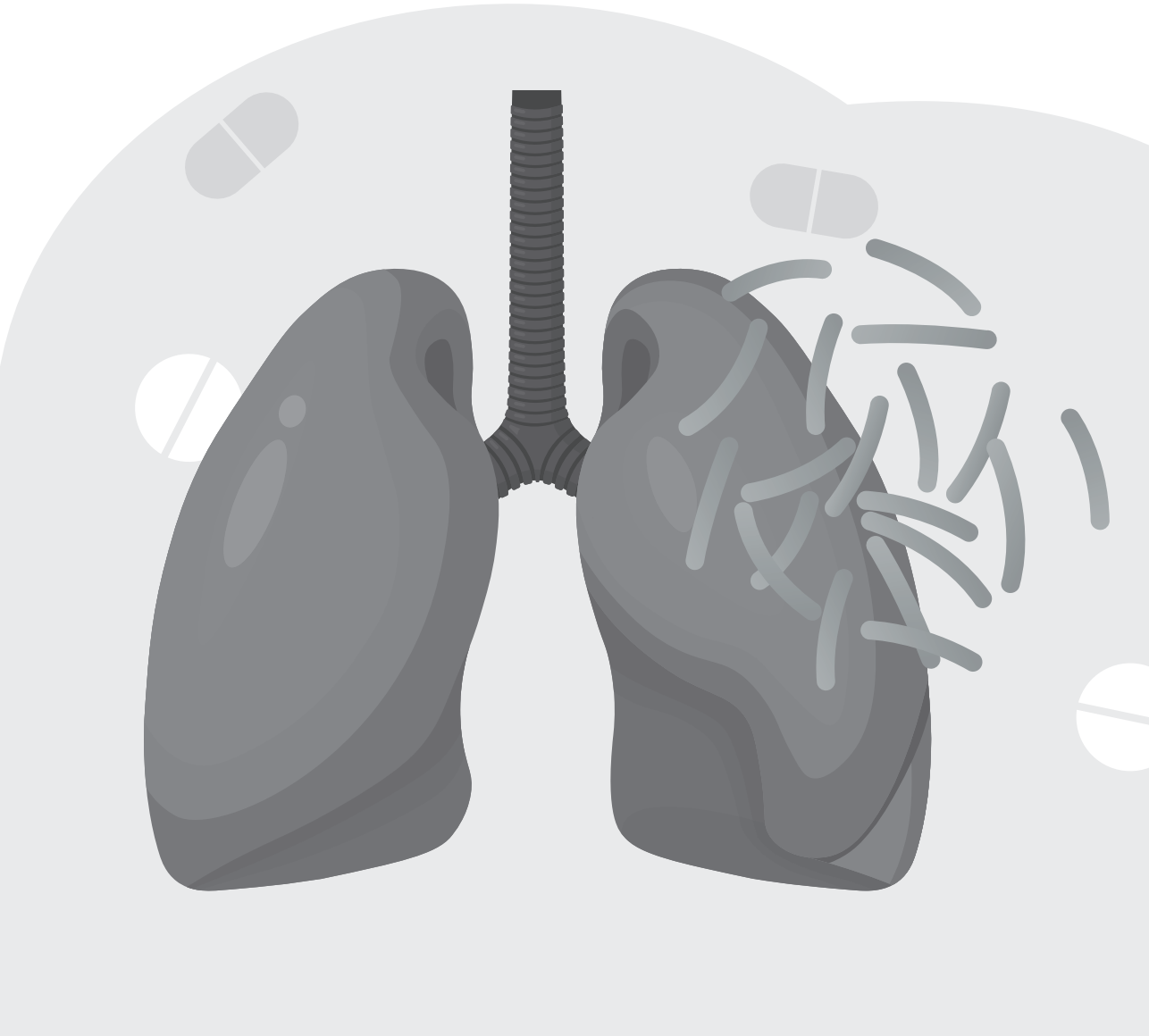

Chapter 2

Optimizing ethambutol dosing among HIV/tuberculosis co-infected patients: a population pharmacokinetic modelling and simulation study

Krina Mehta, Shruthi Ravimohan, Jotam G. Pasipanodya, Shashikant Srivastava, Chawangwa Modongo, Nicola M. Zetola, Drew Weissman, Vijay Ivaturi, Tawanda Gumbo, Gregory P. Bisson, and Christopher Vinnard

J Antimicrob Chemother. 2019 Oct 1;74(10):2994-3002

Abstract

Background: Reduced ethambutol serum concentrations are commonly observed among tuberculosis (TB) patients co-infected with human immunodeficiency virus (HIV) and may lead to treatment failure.

Objectives: To perform a population pharmacokinetic study of ethambutol in HIV/TB patients, and to evaluate an intensified ethambutol weight-based dosing strategy to support pharmacokinetic target attainment.

Methods: We conducted a prospective study of ethambutol pharmacokinetics among HIV/TB patients administered first-line TB treatment in Botswana, with study visits before and after initiation of antiretroviral therapy (ART). Clinical and disease status markers, including HIV-associated systemic immune activation and gut dysfunction biomarkers, were evaluated as covariates of ethambutol pharmacokinetic parameters in non-linear mixed effects analysis. Monte Carlo simulations were performed to compare pharmacokinetic target attainment under standard and intensified weight-based ethambutol dosing strategies.

Results: We studied 40 HIV/TB patients prior to initiation of ART, of whom 24 returned for a second visit a median of 33 days following ART initiation. Ethambutol serum concentrations were best explained by a two-compartment model with first-order elimination, with a significant improvement in oral bioavailability following ART initiation. In Monte Carlo simulations, a supplementary ethambutol dose of 400mg daily led to >2-fold improvements in pharmacokinetic target attainment probabilities in lung tissue, both before and after ART initiation.

Conclusions: Low serum ethambutol concentrations were commonly observed among HIV/TB patients in Botswana, and the oral bioavailability of ethambutol increased following ART initiation. Supplementary ethambutol dosing among HIV/TB patients may provide a strategy to optimize anti-TB treatment regimens in this high-risk population.

Introduction

Ethambutol is a key drug in the first-line TB treatment regimen worldwide, protecting companion drugs against acquired drug resistance and acting synergistically with rifampicin for sterilizing effect in a concentration-dependent fashion.[1-3] More recently, ethambutol has also demonstrated utility in second-line treatment regimens for multi-drug resistant TB (MDR-TB) (caused by Mycobacterium tuberculosis resistant to both isoniazid and rifampicin) in the shortened WHO regimen.[4] Ethambutol demonstrates high partitioning into the center and walls of tuberculous cavities, which likely contributes to its sterilizing effect.[5] Efficacy advantages are counter-balanced by the potential for toxicity, in particular an optic neuritis that is driven by cumulative exposures in a dose-dependent manner.[6-7] However, the mechanism of ethambutol-induced optic neuritis remains undefined, and consequently the optimal strategy for ethambutol dosing among TB patients is uncertain.

Weight-based dosing strategies using fixed-dose combinations of anti-TB drugs are the mainstay of the WHO Global TB Program. These combination regimens were largely developed before the emergence of the HIV epidemic. Administered as daily therapy, ethambutol weight-based dosing bands center around 15–25 mg/kg, without dose adjustment for HIV co-infection or other comorbid diseases. Some, but not all, clinical studies have demonstrated that HIV co-infection is associated with low ethambutol concentrations in peripheral blood.[8-12] Mycobacterial killing by ethambutol is concentration dependent, while prevention of resistance is driven by the proportion of time that ethambutol concentrations persist above the minimum inhibitory concentrations (MIC).[13,14] Thus, low ethambutol exposures may increase the risk of TB treatment failure and the emergence of drug resistance, outcomes that are more commonly observed among TB patients co-infected with HIV.[15,16]

We conducted a prospective study to evaluate the pharmacokinetics of the first-line anti-TB drugs (rifampicin, isoniazid, pyrazinamide and ethambutol) administered via fixed-dose combinations among HIV/TB co-infected patients in Botswana. Here, we report the population pharmacokinetic model of ethambutol, followed by Monte Carlo simulations to identify target attainment probabilities in lung tissue under standard and intensified weight-based dosing strategies.

Methods

Ethics

The study was approved by institutional review boards of the Ministry of Health of Botswana and the University of Pennsylvania. Written informed consent was obtained from all participants.

Study design

We identified ethambutol pharmacokinetic parameters among HIV/TB patients in Gaborone, Botswana, using an intensive pharmacokinetic sampling design. The population pharmacokinetic models for rifampicin, isoniazid and pyrazinamide identified in this study cohort have been previously reported. We measured clinical and disease status markers, including measures of HIV-associated immune activation and gut dysfunction, before and after initiation of ART.

Study population

A detailed description of the study population has been reported.[17] In brief, we enrolled HIV-infected patients >21 years of age who were naive to ART and newly diagnosed with pulmonary TB. We included patients initiated on the standard first-line TB regimen, dosed according to weight-based bands as recommended in WHO guidelines, consistent with the policy of the Botswana National TB Program. Ethambutol was administered as daily therapy according to standard weight-based dosing bands (550 mg if <40kg, 825 mg if 41–55 kg, 1100 mg if 55–70kg, 1375 mg if >70 kg). Exclusion criteria included pregnancy, renal insufficiency (defined as a creatinine clearance (CL_{CR}) <50mL/min) and hepatic dysfunction (defined as either alanine transaminase (ALT) or aspartate transaminase (AST) greater than three times the upper limit of normal).

Data collection

Study procedures included one or two pharmacokinetic study visits for each enrolled patient. The first visit occurred 5–28 days after initiation of standard TB therapy and was performed in each instance prior to the initiation of ART. All participants were eligible to complete a second pharmacokinetic study visit after ART had been initiated. The procedures at both study visits (i.e., pre- and post-ART) were identical. After an overnight fast, the anti-TB drugs were administered by directly observed therapy. Blood samples (10mL) were drawn at 0, 0.3, 0.9, 2.2, 4.5

and 8 h post-dosing, with these timepoints selected according to optimal sampling theory.[20] Clinical and demographic information included age, gender, weight, BMI, serum creatinine, HIV viral load and CD4+ T cell count.

We evaluated additional HIV disease markers as potential covariates related to ethambutol pharmacokinetic variability, including systemic immune activation, microbial translocation and gut dysfunction. HIV associated systemic immune activation was measured as the percentage of CD38+ T cells co-expressing HLA-DR and CD38 (%CD38+DR+CD8+).[21] Other systemic inflammatory markers included plasma levels of neopterin, IL-6 and C-reactive protein (CRP). We also evaluated markers of gut dysfunction related to HIV-associated immune activation, including soluble CD14 (sCD14), a marker of macrophage activation in the LPS pathway,[22] and intestinal fatty acid-binding protein (I-FABP), a measure of intestinal damage.[23]

Analytical methods

Markers of immune activation and gut damage

Blood samples were transported to the Botswana Harvard Partnership Laboratory. We performed plasma and PBMC isolation using Ficoll-Paque Plus (GE Healthcare) density gradient centrifugation. Plasma assays for sCD14, IL-6, neopterin, CRP and I-FABP were performed using previously described methods.[17-19] All assays were performed according to the manufacturers' protocols.

Serum ethambutol concentrations

Cryopreserved serum samples for each timepoint were shipped to the Center for Infectious Diseases Research and Experimental Therapeutics at the Baylor Research Institute (Dallas, TX, USA). We used a previously published stable-isotope dilution LC-electrospray ionization-MS/MS method to determine ethambutol concentrations in the serum.[5] Ethambutol dihydrochloride and the stable isotope (2S,20S)-ethambutol-d10 (1,1,1',1',2,2'-d6; ethylene-d4) were purchased from Sigma–Aldrich (St Louis, MO, USA) and CDN isotopes (Quebec, Canada), respectively. All chemicals used in the assay were chromatographic or LC-MS/MS grade. Calibrators, controls and internal standards (ethambutol-d10) were included in each analytical run for quantification. Quality control samples were prepared by spiking human serum with stock standards (calibration range 0.125–4 mg/L). The lower limit of quantification of this method was 0.16 mg/L with 3.4% intra-day precision.

Statistical analysis

Population pharmacokinetic modelling of ethambutol among HIV/TB patients

Phoenix NLME software 7 (Certara USA, Inc., Princeton, NJ, USA) was used for pharmacokinetic analysis. Summary statistics were obtained for each timepoint, separately for pre- and post-ART visits, and used to explore mean concentration–time plots. Non-compartmental analysis was performed to obtain initial estimates for the pharmacokinetic parameters. The first-order conditional estimation-extended least squares method was used for all population model runs. For nested models, a reduction in the objective function value of >3.84 was considered statistically significant ($P<0.05$), corresponding to a χ^2 distribution with one degree of freedom. We visually examined model goodness of fit by plotting the observed serum ethambutol concentrations versus population-predicted concentrations, observed versus individual-predicted concentrations, individual weighted residuals versus population-predicted concentrations, and conditional weighted residuals versus time.

Standard population pharmacokinetic modelling methodology was applied for model development and evaluations. Oral bioavailability was included in the structural model and fixed to 65% for the first study visit (pre-ART) based on previous findings in HIV/TB-co-infected patients. Prior clinical studies have linked observed variability in ethambutol oral bioavailability to body weight, food intake, genetic factors and disease status. Because we were unable to estimate oral bioavailability in the absence of intravenous dosing data, we fixed this parameter to a previously reported value and estimated interindividual variability (IIV) from this fixed parameter value. This approach allowed us to compare the relative oral bioavailability from one patient to another, even though the absolute bioavailability could not be estimated directly from the data. First-order absorption with lag time (Tlag), transit compartment absorption models and distributional delay models were evaluated. We explored proportional and additive models to describe residual unexplained variability and exponential models to describe IIV. To capture the covariate effect of body weight on ethambutol pharmacokinetic parameters, allometric exponents were either fixed to theoretical values, 0.75 for disposition-related parameters and 1.0 for distribution related parameters, or directly estimated from the data.[24]

Selection of the final population pharmacokinetic model to be used for simulations was based on the Akaike information criterion (AIC), diagnostic plots, plausibility and precision. To evaluate the performance of the final population pharmacokinetic

model, both visual predictive checks and bootstrapping were performed. For the visual predictive checks, the distributions of stochastic simulated ethambutol concentrations (including median and 5th and 95th percentiles) were compared with distributions of the observed concentrations. Differences and overlap of the simulated and original distributions indicated the accuracy of the final model. In the bootstrap analysis, 500 datasets were sampled from the original study dataset. Each of the simulated datasets was fitted to the final model to evaluate variation in predicted parameter estimates (as described by the median and associated 90% CI). Finally, we performed an external validation of the final population pharmacokinetic model, comparing model-simulated serum concentrations with observations from an independent study of 48 HIV/TB patients (not used in model development) treated with daily ethambutol according to standard weight-based dosing guidelines, with the median and range of ethambutol concentrations reported for 2, 6 and 10 h post-dosing.[10]

Monte Carlo simulations of pharmacokinetic target attainment probabilities

Monte Carlo simulations were performed using the RStudio 1.1.383 (RStudio, Boston, MA, USA) platform for software R 3.4.1 (The R Foundation, Vienna, Austria) and R package mrgsolve.[25] Using the pharmacokinetic parameter estimates from the final population pharmacokinetic model (with associated variability), we performed simulations to identify pharmacokinetic target attainment under standard and intensified weight-based dosing strategies.[26] The simulated population contained 1000 virtual patients with normal body weight distribution with mean 55 kg and SD 10 kg.[17] Using the final population model, pharmacokinetic simulations were performed for the standard weight-based dosing regimen as well as an intensified dosing strategy that consisted of a supplementary 400 mg dose across each body weight group, also administered as daily therapy. We selected this intensified treatment strategy based on the ready availability of ethambutol 400 mg oral formulations in TB control programs worldwide. For each virtual patient, we determined AUC0–24 with noncompartmental analysis. Based on prior published data on ethambutol partitioning into pulmonary TB lesions, we estimated a 10-fold increase in lung tissue drug exposures relative to serum drug exposures.[27] We defined the AUC_{0-24}/MIC target ratio in lung tissue as 119, corresponding to EC_{90} in an inhibitory sigmoid E_{max} model of ethambutol pharmacodynamics.[14,28] Since the toxicodynamic relationships of systemic ethambutol exposures remain undefined, we examined the distributions of ethambutol serum C_{max} under standard and intensified dosing strategies in relation to the recommended 'target' ethambutol serum Cmax range of 2–6 mg/L.

Results

A total of 40 patients were enrolled and completed the first pharmacokinetic study visit. Twenty-four patients (60%) returned for a second pharmacokinetic study visit conducted a median of 33 days (range 5–44 days) after starting ART. Among 240 samples collected pre-ART, 8 (3.3%) were below the lower limit of quantification; post-ART, 4 of 144 samples (2.8%) were below the lower limit of quantification. At the time of the second visit, the median duration of anti-TB therapy was 74 days (range 33–118 days). Clinical characteristics for study participants grouped by body weight are shown in **Table 2.1**. Based on the recommended weight-based ethambutol dosing, the first study visit included 1 patient dosed with 550 mg (14.75 mg/kg), 19 patients dosed with 825mg (range 11.77–19.64 mg/kg), 17 patients dosed with 1100 mg (range 16.17–22.92 mg/kg) and 3 patients dosed with 1375 mg (range 17.73–19.31 mg/kg). Serum ethambutol concentration–time profiles, sorted by dose and visit (i.e., pre- or post-ART initiation), are presented in **Figure 2.1**.

Figure 2.1 Individual ethambutol serum concentration–time curves by weight group and study visit, before and after initiation of ART. The weight group 55 kg or lower includes one patient with body weight <40 kg. The horizontal line corresponds to the proposed target range for serum ethambutol Cmax (2–6 mg/L).

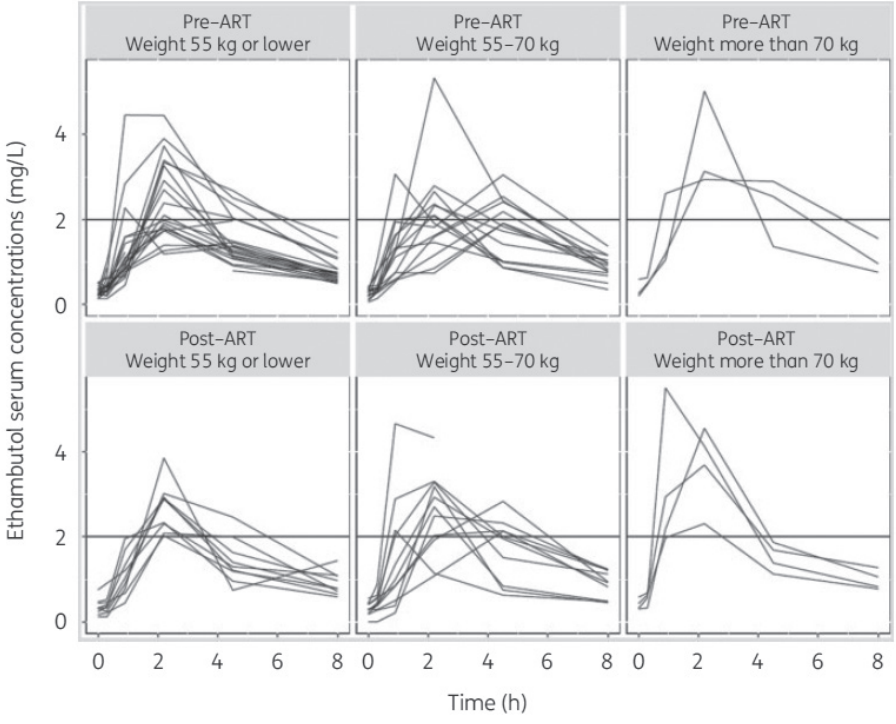

Serum ethambutol concentrations were best described by a two-compartment pharmacokinetic model with first-order absorption with lag time, linear elimination and IIV in the volume of distribution for the central compartment (V1), CL and oral bioavailability. Estimates of IIV in volume of distribution for the peripheral compartment (V2), inter-compartment transfer (Q) and absorption rate constant (ka) were small (<0.0001) and shrinkage in random effects was high, and we did not include IIV in these parameters moving forward in model development. The inclusion of a covariance term between the central compartment volume and CL showed improvement in the model fit based on AIC criteria. A proportional residual variability model adequately described unexplained residual variability. The pharmacokinetic model with fixed allometric exponents on pharmacokinetic parameters (1 for volume parameters, 0.75 for CL parameters) yielded lower AIC values (474.67) than the model with estimated allometric exponents (479.89). Thus, theoretical fixed allometric scaling was used to describe the covariate effect of weight on distribution and CL parameters. Oral bioavailability at the pre-ART study visit was fixed to 0.65[9] and IIV was estimated. Based on the plot of visit effect on IIV in oral bioavailability (S2.1), we evaluated study visit (i.e., pre- or post-ART initiation) as a categorical covariate on oral bioavailability. Interestingly, this effect was found to be statistically significant (-Δ2LL=3.92), and therefore was retained in the final model. We sequentially evaluated serum creatinine, HIV viral load, CD4+ T cell count, % CD8+CD38+DR+, neopterin, IL-6, CRP, sCD14 and I-FABP as covariates on CL and oral bioavailability. None of these covariate effects reached our pre-defined criteria for statistical significance, and thus were not retained in the final model. Parameter estimates from the final population pharmacokinetic model are shown in **Table 2.2**. Overall, parameter estimates were plausible and comparable to those previously reported in other studies[9,11,24] with a coefficient of variation, 25% for most parameters. The goodness of fit of the final model was supported by diagnostic plots (S2.2).

Table 2.1 Summary of clinical characteristics (median and IQR) by body weight group.

	HIV/TB patient body weight category		
	>55 kg (n=22)[a]	**55–70 kg (n=15)**	**<70 kg (n=3)**
Creatinine (μmol/L)	64.7 (55.4–69.1)	69.0 (60.9–73.2)	64.3 (58.0–65.1)
Age (years)	32 (27.2–43.5)	31 (27–34)	46 (39–47)
IL6 (pg/mL)	15.1 (9.15–29.1)	16.6 (8.2–26.7)	4.6 (4.4–5.9)
sCD14 (μg/mL)	2.5 (2.0–3.8)	3.2 (2.8–4.0)	3.1 (3.0–3.3)
I-FABP (pg/mL)	407.7 (188.4–573.8)	179.9 (74.9–506.6)	327.2 (306.5–424.4)
CD4 count (cells/mm^3)	217 (94.75–320)	237 (139.5–305)	352 (301–425)
Neopterin (ng/mL)	10.9 (6.68–14.8)	10.7 (7.0–20.1)	7.1 (6.3–7.8)
CRP (μg/mL)	15.2 (3.5–35.7)	7.5 (4.0–12.8)	8.3 (6.0–9.7)
CD8+CD38+DR+ (%)	38.5 (28.1–45.7)	38.5 (27.7–53.3)	27.6 (27.4–31.5)
Viral load (log_{10} copies/mL)	11.4 (10.3–13.0)	11.3 (10.0–13.3)	10.4 (10.1–12.1)
Female gender, n (%)	10 (45%)	5 (33%)	3 (100%)

[a] Includes one patient with body weight ,40 kg.

Table 2.2 Parameter estimates from the final ethambutol population pharmacokinetic model.

Population pharmacokinetic parameters	**Typical value (% SE)**	**Median (95% CI)[a]**
k_a (h$^{\#1}$)	0.44 (19.80)	0.42 (0.31–0.59)
T_{lag} (h)	0.25 (3.09)	0.26 (0.24–0.27)
Oral bioavailability for pre-ART visit (*F*)	0.65 (fixed)	0.65 (fixed)
Change in oral bioavailability post-ART	0.12 (54.45)	0.13 (0.00052–0.25)
V_1 (L)	110.23 (20.78)	107.05 (71.52–151.35)
CL (L/h)	35.42 (4.64)	35.56 (32.73–38.20)
V_2 (L)	512.52 (54.01)	634.82 (313.46–3784.53)
Q (L/h)	27.25 (16.08)	25.66 (19.62–34.28)
Weight exponent for CL and *Q*	0.75 (fixed)	0.75 (fixed)
Weight exponent for V_1 and V_2	1 (fixed)	1 (fixed)
IIV		
in *F* (%)	10.00 (13.61)	11.09 (9.04–12.91)
in V_1 (%)	55.67 (23.35)	54.27 (29.89–78.11)
in CL (%)	14.14 (5.65)	13.41 (11.92–14.89)
Residual unexplained variability		
proportional (%)	36.00 (6.10)	35.16 (31.32–39.31)

[a] Obtained from bootstrap of 1000 replicates.

Visual predictive checks from the final model demonstrate adequate model fit with the observed data (S2.3). Once the final pharmacokinetic model was identified,

we performed Monte Carlo simulations of serum ethambutol concentration–time profiles. We first simulated ethambutol serum concentrations under the standard-of-care weight-based dosing scheme. For each virtual patient, we sampled from distributions of body weight, assigning ethambutol dose based on WHO guidelines, as described above. We performed an external validation of the pharmacokinetic model by comparing simulated serum ethambutol concentrations at 2, 6 and 10 h post-dosing with observed serum ethambutol concentrations at these timepoints, as reported in a separate pharmacokinetic study among HIV/TB patients that was not used in model development.[10] The overlap between distributions of simulated and observed serum ethambutol concentrations at these timepoints supported the use of the pharmacokinetic model for simulation purposes **(Figure 2.2)**.

Figure 2.2 External validation of pharmacokinetic model, comparing simulated and observed distributions of serum ethambutol concentrations at 2, 6 and 10 h post-dosing with observed values reported in a cohort of 48 HIV/tuberculosis patients.[10] The box represents the 25th–75th quartiles, the solid horizontal line in the box represents the arithmetic mean, and the error bars represent 1.5%IQR. The floating bars represent the range of observed serum ethambutol concentrations at each timepoint.

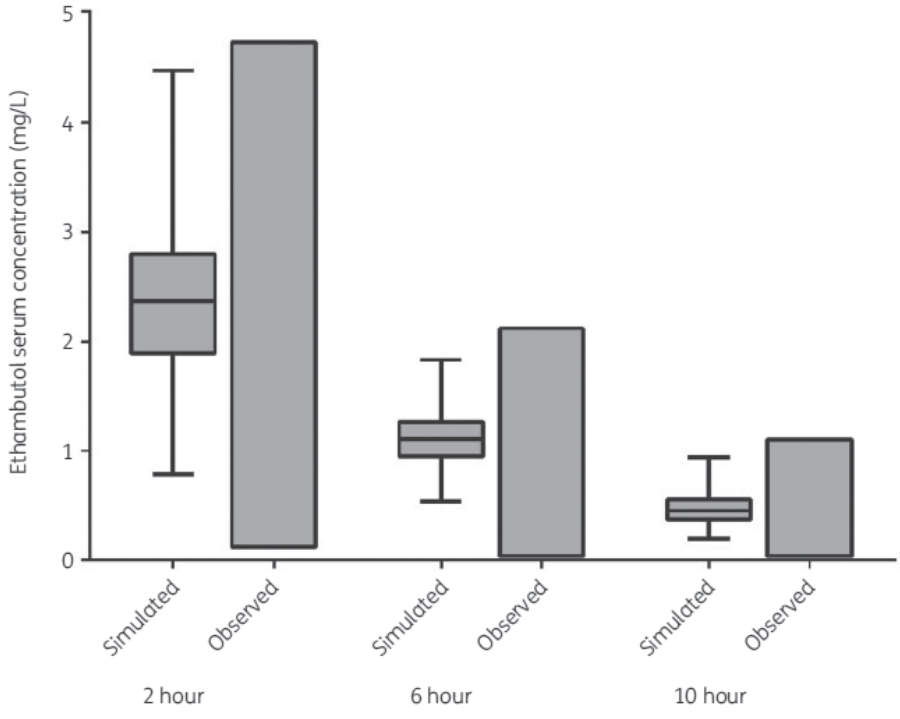

Next, we estimated probabilities of ethambutol pharmacokinetic target attainment in lung tissue according to ethambutol MIC values, under standard and intensified dosing strategies. The lung tissue AUC0–24 was estimated from the reported partitioning of ethambutol into pulmonary lesions[27] and the ethambutol MIC for the infecting *Mycobacterium tuberculosis* (Mtb) strain was sampled from a previously reported MIC distribution of ethambutol-susceptible strains.[30] The probabilities of successful pharmacokinetic target attainment at each MIC level, defined as a ratio of ethambutol AUC0–24/MIC in lung tissue >119, are shown in **Figure 2.3**. We separately compared probabilities of pharmacokinetic target attainment under standard and intensified dosing strategies among HIV/TB patients pre-ART **(Figure 2.3a)** and post-ART **(Figure 2.3b)**.

Figure 2.3 Probability of pharmacokinetic target attainment under standard and intensified ethambutol dosing strategies (n=1000 per simulation). The pharmacokinetic target was defined as an AUC0–24/MIC ratio in lung tissue .119. Circles/solid line, standard dosing regimen; squares/dashed line, intensified dosing regimen. (a) Before initiation of ART. (b) After initiation of ART.

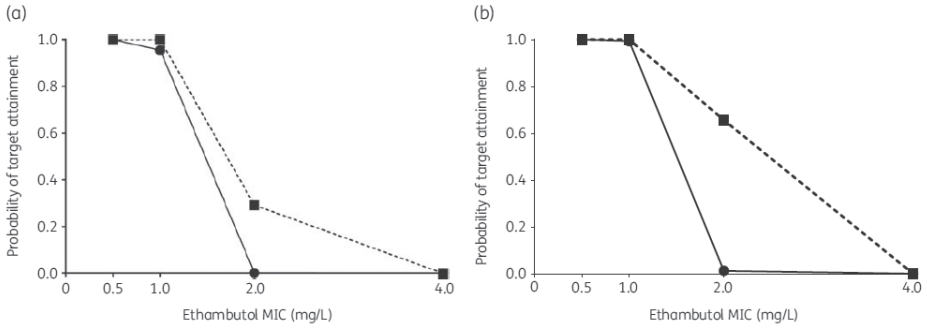

Figure 2.4 Comparison of ethambutol (EMB) pharmacokinetic target attainment probabilities by body weight category, before (a) and after (b) initiation of ART (n=1000 per simulation).

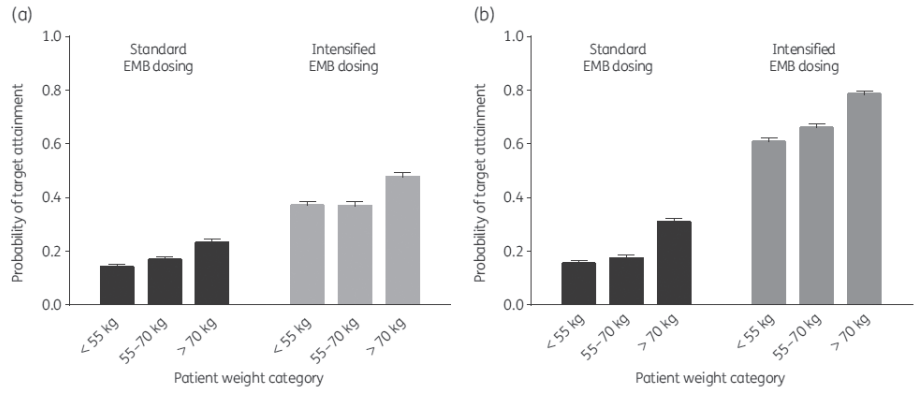

The cumulative fraction of response pre-ART under standard dosing was 15.8% and under intensified dosing was 37.6%. Post-ART initiation, the cumulative fraction of response was 17.2% under standard dosing and 64.1%with intensified dosing. Notably, at the ethambutol MIC level of 4mg/L, the PTA was <1% across all scenarios. Patients in the lowest body weight category (under 55 kg) were least likely to demonstrate pharmacokinetic target attainment under each simulation scenario, both before (**Figure 2.4a)** and after **(Figure 2.4b)** ART initiation. Finally, in order to characterize the safety of intensified ethambutol dosing, we determined the proportion of virtual patients achieving ethambutol serum Cmax between 2 and 6mg/L, the recommended range for clinicians in the context of therapeutic drug monitoring.[29] Under an intensified dosing strategy, the ethambutol serum Cmax fell between 2 and 6mg/L for 94% of virtual patients pre-ART initiation and 97% post-ART initiation. Among the 9% of virtual patients with ethambutol serum Cmax outside the target range post-ART initiation, 8% were, 2mg/L and 1% were .6mg/L, with similar proportions in each body weight category **(Figure 2.5)**. Thus, this intensified dosing strategy did not lead to supratherapeutic serum ethambutol exposures in these simulations, as defined by the recommended range of peak serum concentrations.

Figure 2.5 Simulation-based evaluation of the proportion of virtual HIV/TB patients with serum ethambutol Cmax within the proposed target range under an intensified dosing strategy, according to body weight category (n=1000 per simulation). The grey and black lines correspond to simulated patients with peak serum ethambutol within and outside of the target range, respectively.

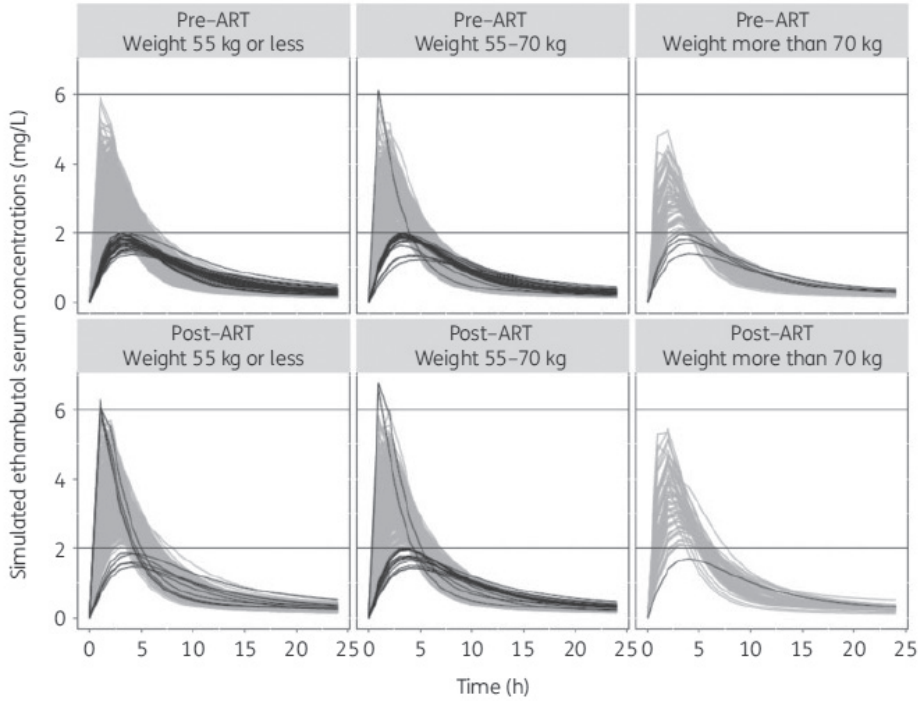

Discussion

Ethambutol remains a key drug in the first-line treatment regimen for TB. Prior work has demonstrated that HIV co-infection exerts a negative effect on ethambutol oral bioavailability, with a 15% reduction in oral bioavailability among TB patients co-infected with HIV, compared with HIV-uninfected TB patients.[9] Our work builds on these findings with the novel observation that ART initiation restores, at least partially, ethambutol oral bioavailability among HIV/TB patients treated with standard dosing regimens. We were unable to identify a specific HIV disease biomarker that was associated with improvement in oral bioavailability, among virological, immunological or gut-specific measures of HIV disease. Indeed, we cannot rule out that an overall improvement in health status, as a consequence of HIV and TB treatment, led to the increase in oral bioavailability. Broadly, these findings support efforts to identify the optimal strategy for managing HIV/TB patients who are ART naive at the time of TB treatment initiation.[31] Future work should identify mechanisms for the observed effect of ART initiation on ethambutol

oral bioavailability, whether driven by drug–drug interactions (for example, effects of ART) or drug–disease interactions (as we have demonstrated with effects of HIV-associated immune activation on the CL of isoniazid[17] and pyrazinamide[18]).

Monte Carlo simulations with our population pharmacokinetic model demonstrated that an intensified dosing strategy, comprising a supplementary dose of 400mg across all body weight groups, led to improvements in pharmacokinetic target attainment in lung tissue (measuring efficacy) while maintaining the serum Cmax range within the recommended range (approximating safety). The benefit of intensified ethambutol dosing was most notable for Mtb strains at an ethambutol MIC of 2mg/L, with an increase in target attainment probability from ,1% to 29% (pre-ART), and from 1% to 65% (post-ART). Based on these findings, the combination of early ART and intensified ethambutol dosing appears essential to achieve >50% probability of efficacious exposures to ethambutol in infected lung tissue among HIV/TB patients.

An additional finding of the current work was that the ethambutol MIC of 4mg/L provided an unattainable pharmacokinetic target for HIV/TB patients (both pre- and post-ART) under both the standard and intensified dosing strategies. This is particularly notable given the increasing recognition that the susceptibility breakpoints for anti-TB drugs should reflect the probability of pharmacokinetic target attainment during treatment.[28,32] These findings should be validated in prospective cohorts of HIV/TB patients, in order to relate these pharmacokinetic/pharmacodynamic indices to clinical endpoints (such as time to sterilization of sputum samples).[33]

A previous pharmacokinetic study conducted among healthy volunteers demonstrated that the ethambutol AUC0–24 was significantly lower among obese (BMI 25–40 kg/m^2) and extremely obese (BMI>40 kg/ m^2) individuals compared with individuals with a BMI <25 kg/m^2.[2.24] Although we were unable to characterize the effects of obesity on ethambutol pharmacokinetics given the body weight distribution of the study population, the current WHO weight-based bands for ethambutol dosing may require further optimization among patients with increased BMI in order to reach serum targets. Similarly, the absence of patients with significant kidney disease in the study cohort constrained our ability to study this covariate effect on CL, even though ethambutol is renally eliminated. The effects of BMI and kidney disease on ethambutol pharmacokinetics require further investigation given the merging of HIV, diabetes mellitus and TB epidemics, and the increasing need to treat overweight or obese patients with optimized ethambutol dosing.[34]

Our study had several limitations. First, the study was not designed to evaluate safety endpoints such as optic neuritis that may be associated with increasing ethambutol exposures,[6,7,35] and serum Cmax values within a recommended range were used as an approximate measure of the safety of an intensified dosing scheme. Although many of the early clinical studies of ethambutol included much higher dosing than currently used (up to 50mg/kg), optic neuritis can develop with doses as low as 15mg/kg and may occur more commonly among patients with nutritional deficiencies.[36] As with the other first-line anti-TB drugs, delineating toxicodynamic relationships will be essential to support intensified dosing strategies among high-risk patients.[37] In addition, we estimated lung tissue drug exposure relative to serum based on the rabbit model of tuberculous lung lesions[27], which may overestimate ethambutol exposures at the center of lung cavities and underestimate ethambutol exposures in alveolar cells.[38] Furthermore, the ethambutol MIC demonstrates regional variability in tuberculous lung lesions,[5] which adds additional complexity to the likelihood of AUC0–24/MIC target attainment. Although the pharmacodynamic target was identified in the hollow-fiber system, which provides the basis for dose selection in TB drug development guidance from both the FDA and EMA, emerging clinical data should validate this target. Finally, because pharmacokinetic sampling was limited to the central compartment, we were unable to incorporate additional IIV in ethambutol partitioning into lung tissue in Monte Carlo simulations of target attainment probabilities. Strengths of the study include the multifaceted characterization of HIV disease status (including immunological, virological and gut-specific assays) and the repeated measures study design, supporting the formal investigation of the effects of ART initiation on ethambutol pharmacokinetics during TB treatment.

In summary, we present the novel finding that ART initiation among HIV/TB-co-infected patients was associated with an improvement in ethambutol oral bioavailability and provide evidence in support of the efficacy and safety of an intensified ethambutol dosing strategy to optimize ethambutol use among HIV/TB patients. Given the critical role of ethambutol in TB treatment regimens, emerging knowledge regarding the pharmacokinetic/pharmacodynamic indices of ethambutol safety and efficacy will support further refinement of treatment strategies among high-risk TB patient populations.

References

1. Nahid P, Dorman SE, Alipanah N et al. Official American Thoracic Society/Centers for Disease Control and Prevention/Infectious Diseases Society of America Clinical Practice Guidelines: Treatment of Drug-Susceptible Tuberculosis. Clin Infect Dis 2016; 63: e147–e95.
2. Mitchison DA. Role of individual drugs in the chemotherapy of tuberculosis. Int J Tuberc Lung Dis 2000; 4: 796–806.
3. Chigutsa E, Pasipanodya JG, Visser ME et al. Impact of nonlinear interactions of pharmacokinetics and MICs on sputum bacillary kill rates as a marker of sterilizing effect in tuberculosis. Antimicrob Agents Chemother 2015; 59: 38–45.
4. Caminero JA, Sotgiu G, Zumla A et al. Best drug treatment for multidrug-resistant and extensively drug-resistant tuberculosis. Lancet Infect Dis 2010; 10: 621–9.
5. Dheda K, Lenders L, Magombedze G et al. Drug penetration gradients associated with acquired drug resistance in tuberculosis patients. Am J Respir Crit Care Med 2018; 198: 1208–19.
6. Leibold JE. The ocular toxicity of ethambutol and its relation to dose. Ann N Y Acad Sci 1966; 135: 904–9.
7. Harcombe A, Kinnear W, Britton J et al. Ocular toxicity of ethambutol. Respir Med 1991; 85: 151–3.
8. Sahai J, Gallicano K, Swick L et al. Reduced plasma concentrations of anti- tuberculosis drugs in patients with HIV infection. Ann Intern Med 1997; 127: 289–93.
9. Jonsson S, Davidse A, Wilkins J et al. Population pharmacokinetics of ethambutol in South African tuberculosis patients. Antimicrob Agents Chemother 2011; 55: 4230–7.
10. Perlman DC, Segal Y, Rosenkranz S et al. The clinical pharmacokinetics of rifampin and ethambutol in HIV-infected persons with tuberculosis. Clin Infect Dis 2005; 41: 1638–47.
11. Denti P, Jeremiah K, Chigutsa E et al. Pharmacokinetics of isoniazid, pyrazinamide, and ethambutol in newly diagnosed pulmonary TB patients in Tanzania. PLoS One 2015; 10: e0141002.
12. Van Oosterhout JJ, Dzinjalamala FK, Dimba A et al. Pharmacokinetics of antituberculosis drugs in HIV-positive and HIV-negative adults in Malawi. Antimicrob Agents Chemother 2015; 59: 6175–80.
13. Deshpande D, Srivastava S, Meek C et al. Ethambutol optimal clinical dose and susceptibility breakpoint identification by use of a novel pharmacokinetic-pharmacodynamic model of disseminated intracellular Mycobacterium avium. Antimicrob Agents Chemother 2010; 54: 1728–33.
14. Srivastava S, Musuka S, Sherman C et al. Efflux-pump-derived multiple drug resistance to ethambutol monotherapy in Mycobacterium tuberculosis and the pharmacokinetics and pharmacodynamics of ethambutol. J Infect Dis 2010; 201: 1225–31.
15. Li J, Munsiff SS, Driver CR et al. Relapse and acquired rifampin resistance in HIV-infected patients with tuberculosis treated with rifampin- or rifabutin- based regimens in New York City, 1997-2000. Clin Infect Dis 2005; 41: 83–91.
16. Korenromp EL, Scano F, Williams BG et al. Effects of human im- munodeficiency virus infection on recurrence of tuberculosis after rifampin-based treatment: an analytical review. Clin Infect Dis 2003; 37: 101–12.
17. Vinnard C, Ravimohan S, Tamuhla N et al. Isoniazid clearance is impaired among human immunodeficiency virus/tuberculosis patients with high levels of immune activation. Br J Clin Pharmacol 2017; 83: 801-11.
18. Vinnard C, Ravimohan S, Tamuhla N et al. Pyrazinamide clearance is impaired among HIV/tuberculosis patients with high levels of systemic immune activation. PLoS One 2017; 12: e0187624.
19. Vinnard C, Ravimohan S, Tamuhla N et al. Markers of gut dysfunction do not explain low rifampicin bioavailability in HIV-associated TB. J Antimicrob Chemother 2017; 72: 2020.
20. Tam VH, Preston SL, Drusano GL. Optimal sampling schedule design for populations of patients. Antimicrob Agents Chemother 2003; 47: 2888–91.

21. Giorgi JV, Liu Z, Hultin LE et al. Elevated levels of CD38! CD8! T cells in HIV infection add to the prognostic value of low CD4+ T cell levels: results of 6 years of follow-up. The Los Angeles Center, Multicenter AIDS Cohort Study. JAcquir Immune Defic Syndr 1993; 6: 904–12.

22. Sandler NG, Wand H, Roque A et al. Plasma levels of soluble CD14 inde- pendently predict mortality in HIV infection. J Infect Dis 2011; 203: 780–90.

23. Perkins MR, Bartha I, Timmer JK et al. The interplay between host genetic variation, viral replication, and microbial translocation in untreated HIV- infected individuals. J Infect Dis 2015; 212: 578–84.

24. Hall RG 2nd, Swancutt MA, Meek C et al. Ethambutol pharmacokinetic variability is linked to body mass in overweight, obese, and extremely obese people. Antimicrob Agents Chemother 2012; 56: 1502–7.

25. Baron KT, Gastonguay MR, Simulation from ODE-based population PK/PD and systems pharmacology models in R with mrgsolve. J Pharmacokinet Pharmacodyn 2015; W-23: S84–5.

26. Pasipanodya J, Gumbo T. An oracle: antituberculosis pharmacokinetics-pharmacodynamics, clinical correlation, and clinical trial simulations to predict the future. Antimicrob Agents Chemother 2011; 55: 24–34.

27. Zimmerman M, Lestner J, Prideaux B et al. Ethambutol partitioning in tuberculous pulmonary lesions explain its clinical efficacy. Antimicrob Agents Chemother 2017; 61: e00924-17.

28. Gumbo T. New susceptibility breakpoints for first-line antituberculosis drugs based on antimicrobial pharmacokinetic/ pharmacodynamic science and population pharmacokinetic variability. Antimicrob Agents Chemother. 2010; 54: 1484–91.

29. Alsultan A, Peloquin CA. Therapeutic drug monitoring in the treatment of tuberculosis: an update. Drugs 2014; 74: 839–54.

30. Schon T, Jure´en P,Giske CGet al. Evaluation ofwild-type MIC distributions as a tool for determination of clinical breakpoints for Mycobacteriumtuberculosis. J Antimicrob Chemother 2009; 64: 786–93.

31. US Department of Health and Human Services. Guidelines for the Use of Antiretroviral Agents in Adults and Adolescents Living with HIV. https://aidsinfo.nih.gov/contentfiles/ lvguidelines/AdultandAdolescentGL.pdf.

32. Gumbo T, Angulo-Barturen I, Ferrer-Bazaga S. Pharmacokinetic-pharmacodynamic and dose–response relationships of antituberculosis drugs: recommendations and standards for industry and academia. J Infect Dis 2015; 211: S96–S106.

33. Magombedze G, Pasipanodya JG, Srivastava S et al. Transformation morphisms and time-to-extinction analysis thatmap therapy duration from preclinical models to patients with tuberculosis: translating from apples to oranges. Clin Infect Dis 2018; 67: S349–S358.

34. Jeon CY,MurrayMB. Diabetes mellitus increases the risk of active tuberculosis: a systematic review of 13 observational studies. PLoS Med 2008; 5: e152.

35. Ezer N, Benedetti A, Darvish-Zargar M et al. Incidence of ethambutol related visual impairment during treatment of active tuberculosis. Int J Tuberc Lung Dis 2013; 17: 447–55.

36. Koul PA. Ocular toxicity with ethambutol therapy: timely recaution. Lung India 2015; 32: 1–3.

37. Srivastava S, Deshpande D, Magombedze G et al. Efficacy versus hepatotoxicity of high-dose rifampin, pyrazinamide, and moxifloxacin to shorten tuberculosis therapy duration: there is still a fight in the old warriors yet! Clin Infect Dis 2018; 67: S359–S364.

38. Conte JE, Golden JA, Kipps J et al. Effects of AIDS and gender on steady-state plasma and intrapulmonary ethambutol concentrations. Antimicrob Agents Chemother 2001; 45: 2891–6.

Supplementary Materials

Figure S2.1. IIV (Eta) in bioavailability by visits, before (Figure 1a) and after (Figure 1b) the inclusion of study visit as a covariate on oral bioavailability. The box represents 25th and 75th quartiles, solid horizontal line in box represent arithmetic mean, dashed horizontal line in box represent median, and the error bars represent 1.5 x interquartile range.

(a)

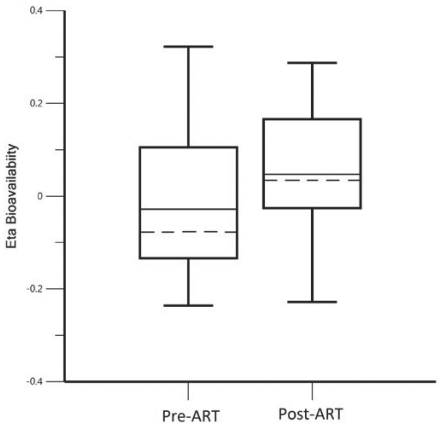

(b)

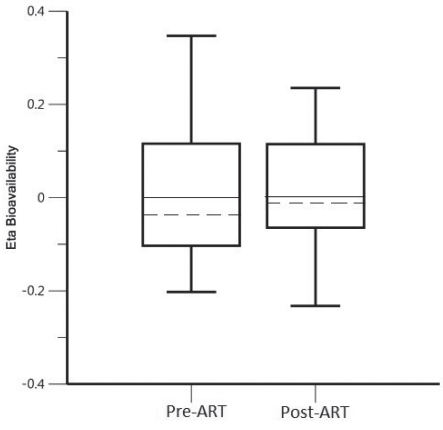

Figure S2.2. Diagnostics plots from final ethambutol population pharmacokinetic model. (a) observed versus individual predicted concentrations, Black dots: Observed, Solid line: linear regression line; (b) conditional weighted residuals versus individual variable (time after dose), Black dots: Observed, Solid line: Loess regression; (c) conditional weighted residuals versus population predicted concentrations, Black dots: Observed, Solid line: loess regression.

(a)

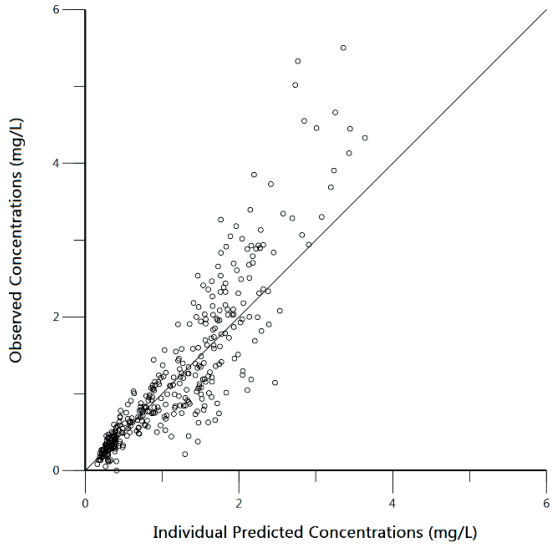

(b)

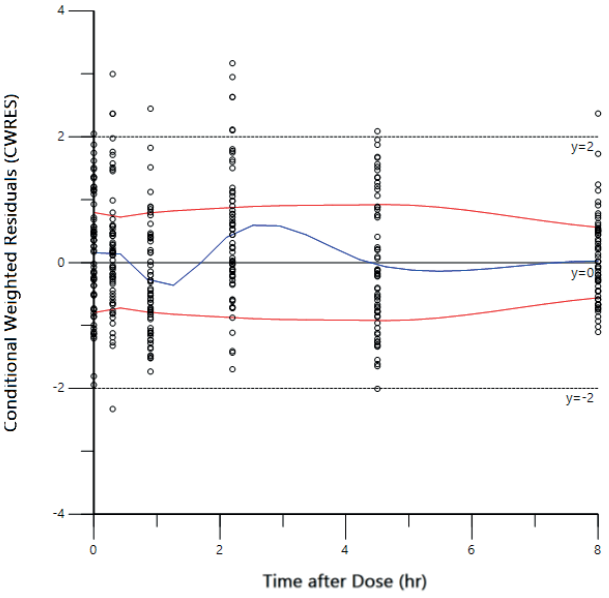

(c)

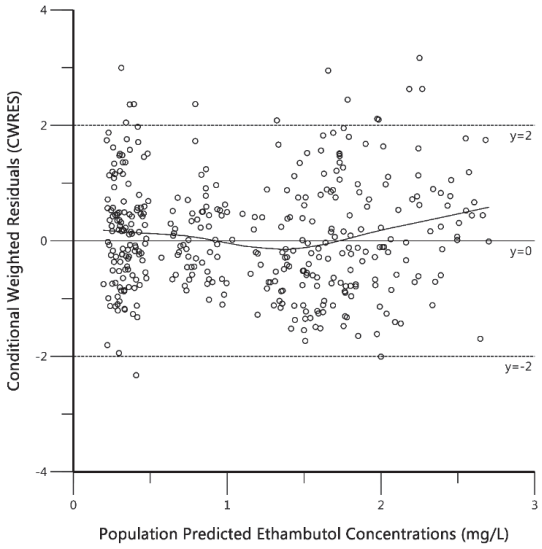
Conditional Weighted Residuals (CWRES)
Population Predicted Ethambutol Concentrations (mg/L)
y=2
y=0
y=-2
4
2
0
-2
-4
0
1
2
3

Figure S2.3. Prediction corrected visual predictive checks from 500 replicates of final ethambutol population pharmacokinetic model. Gray dots: observed, Gray lines: observed 5th, 50th, 95th quantiles; black dotted lines: 95% CI for predicted quantiles (5th, 50th, and 95th), black solid and dashed lines: 50th quantiles of respective predicted quantiles.